



Increased functional connectivity of the intraparietal sulcus underlies the attenuation of numerosity estimations for self-generated words

Giedre Stripeikyte, Michael Pereira, Giulio Rognini, Jevita Potheegadoo, Olaf Blanke, Nathan Faivre

► To cite this version:

Giedre Stripeikyte, Michael Pereira, Giulio Rognini, Jevita Potheegadoo, Olaf Blanke, et al.. Increased functional connectivity of the intraparietal sulcus underlies the attenuation of numerosity estimations for self-generated words. Journal of Neuroscience, 2021, pp.JN-RM-3164-20. 10.1523/JNEUROSCI.3164-20.2021 . hal-03341909

HAL Id: hal-03341909

<https://hal.science/hal-03341909>

Submitted on 13 Oct 2021

HAL is a multi-disciplinary open access archive for the deposit and dissemination of scientific research documents, whether they are published or not. The documents may come from teaching and research institutions in France or abroad, or from public or private research centers.

L'archive ouverte pluridisciplinaire **HAL**, est destinée au dépôt et à la diffusion de documents scientifiques de niveau recherche, publiés ou non, émanant des établissements d'enseignement et de recherche français ou étrangers, des laboratoires publics ou privés.

Research Articles: Behavioral/Cognitive

Increased functional connectivity of the intraparietal sulcus underlies the attenuation of numerosity estimations for self-generated words

<https://doi.org/10.1523/JNEUROSCI.3164-20.2021>

Cite as: J. Neurosci 2021; 10.1523/JNEUROSCI.3164-20.2021

Received: 18 December 2020

Revised: 29 June 2021

Accepted: 1 July 2021

This Early Release article has been peer-reviewed and accepted, but has not been through the composition and copyediting processes. The final version may differ slightly in style or formatting and will contain links to any extended data.

Alerts: Sign up at www.jneurosci.org/alerts to receive customized email alerts when the fully formatted version of this article is published.

Copyright © 2021 the authors

**Increased functional connectivity of the intraparietal sulcus underlies the
attenuation of numerosity estimations for self-generated words**

Abbreviated title: Attenuation of numerosity estimations

Authors

Giedre Stripeikyte^{1,2}, Michael Pereira^{1,2,3}, Giulio Rognini^{1,2}, Jevita Potheegadoo^{1,2}, Olaf Blanke^{1,2,4*}, Nathan Faivre^{1,2,3*}

Affiliations

1. Center for Neuroprosthetics, Swiss Federal Institute of Technology (EPFL), CH-1202 Geneva, Switzerland
2. Brain Mind Institute, Faculty of Life Sciences, Swiss Federal Institute of Technology (EPFL), CH-1015 Lausanne, Switzerland
3. Univ. Grenoble Alpes, Univ. Savoie Mont Blanc, CNRS, LPNC, 38000 Grenoble, France
4. Department of Neurology, University of Geneva, CH-1211 Geneva, Switzerland

* These authors contributed equally to this study

Corresponding authors

Olaf Blanke
Bertarelli Chair in Cognitive Neuroprosthetics
Center for Neuroprosthetics & Brain Mind Institute
School of Life Sciences
Campus Biotech
Swiss Federal Institute of Technology
Ecole Polytechnique Fédérale de Lausanne (EPFL)
CH – 1202 Geneva
E-mail: olaf.blanke@epfl.ch

Nathan Faivre
Laboratoire de Psychologie et Neurocognition
CNRS UMR 5105, UGA BSHM
1251 Avenue Centrale, 38058 Grenoble Cedex 9, France
E-mail: nathan.faivre@univ-grenoble-alpes.fr

Number of pages: 43

Number of figures: 7; **tables:** 4

Number of words abstract: 194; **introduction:** 647; **discussion:** 1498

Conflict of interest statement

The authors declare no competing interests.

42 **ABSTRACT**

43 Previous studies have shown that self-generated stimuli in auditory, visual, and
44 somatosensory domains are attenuated, producing decreased behavioral and neural
45 responses compared to the same stimuli that are externally generated. Yet, whether such
46 attenuation also occurs for higher-level cognitive functions beyond sensorimotor processing
47 remains unknown. In this study, we assessed whether cognitive functions such as
48 numerosity estimations are subject to attenuation in 56 healthy participants (32 women).
49 We designed a task allowing the controlled comparison of numerosity estimations for self
50 (active condition) and externally (passive condition) generated words. Our behavioral results
51 showed a larger underestimation of self- compared to externally-generated words,
52 suggesting that numerosity estimations for self-generated words are attenuated. Moreover,
53 the linear relationship between the reported and actual number of words was stronger for
54 self-generated words, although the ability to track errors about numerosity estimations was
55 similar across conditions. Neuroimaging results revealed that numerosity underestimation
56 involved increased functional connectivity between the right intraparietal sulcus and an
57 extended network (bilateral supplementary motor area, left inferior parietal lobule and left
58 superior temporal gyrus) when estimating the number of self vs. externally generated
59 words. We interpret our results in light of two models of attenuation and discuss their
60 perceptual versus cognitive origins.

61

62 **SIGNIFICANCE STATEMENT**

63 We perceive sensory events as less intense when they are self-generated compared to
64 externally-generated ones. This phenomenon, called attenuation enables us to distinguish
65 sensory events from self and external origins. Here, we designed a novel fMRI paradigm to
66 assess whether cognitive processes such as numerosity estimations are also subject to
67 attenuation. When asking participants to estimate the number of words they had generated
68 or passively heard, we found bigger underestimation in the former case, providing
69 behavioral evidence of attenuation. Attenuation was associated with increased functional
70 connectivity of the intraparietal sulcus, a region involved in numerosity processing.
71 Together, our results indicate that attenuation of self-generated stimuli is not limited to
72 sensory consequences but also impact cognitive processes such as numerosity estimations.

73

74 **INTRODUCTION**

75 The ability to distinguish self- versus externally-generated stimuli is crucial for self-
 76 representation (Kircher and David, 2003; Legrand, 2006). A typical mechanism by which
 77 stimuli generated by oneself and those caused by external sources are distinguished is
 78 sensory attenuation, whereby self-generated stimuli are perceived as less intense. Indeed,
 79 previous studies have shown that self-produced stimuli in the auditory (Baess et al., 2011;
 80 Timm et al., 2014), visual (Hughes and Waszak, 2011; Benazet et al., 2016) and
 81 somatosensory domains (Shergill et al., 2013; Kilteni and Ehrsson, 2020), are perceived as
 82 less intense compared to the same stimuli when they are externally generated. Such
 83 attenuation was shown at the behavioral level and at the neural level in sensory cortical
 84 regions (e.g., auditory cortex (Rummell et al., 2016; Whitford, 2019)) as well as the
 85 thalamus, cerebellum, supplementary motor area and inferior parietal cortex (Hickok, 2012;
 86 Lima et al., 2016; Bansal et al., 2018; Brooks and Cullen, 2019).

87

88 Previous studies have shown that attenuation not only applies to stimuli that are generated
 89 by overt actions, but also extends to covert processes such as motor imagery (Kilteni et al.,
 90 2018) or inner speech (Scott et al., 2013; Whitford et al., 2017). In the latter case,
 91 attenuation of the electrophysiological (Whitford et al., 2017; Jack et al., 2019) and
 92 behavioral (Scott et al., 2013) responses corresponding to the test stimulus (phoneme) was
 93 observed when it matched the imagined cued phoneme. These studies used phonemes that
 94 are integrated into the early stages of hierarchical speech processing implying primary
 95 sensory cortices (Liebenthal et al., 2005; DeWitt and Rauschecker, 2012), where attenuation
 96 effects have been demonstrated (Rummell et al., 2016). An outstanding question is whether

97 attenuation of self-generated stimuli is limited to sensory consequences (e.g., weakened
98 percept) or whether it can also impact cognitive processes that are non-perceptual in nature
99 such as abstract judgments or performance monitoring.

100 To answer this question, we investigated the cognitive function of numerosity estimations,
101 defined as approximate judgments when counting is not involved (Dehaene, 1997).

102 Properties of numerosity estimations such as innateness, amodality, or precision that
103 linearly decreases with increasing numerosity have been described (Anobile et al., 2016;
104 Burr et al., 2018). Extensive neuroimaging work has also established that brain areas in the
105 intraparietal sulcus (IPS) region play a key role in numerosity processing (for review, see
106 Arsalidou & Taylor, 2011). If attenuation for self-related functions extends to higher-level
107 cognitive processes such as numerosity estimations, we would expect the number of items
108 that are self-generated to be underestimated compared to externally-generated items in
109 relation to modulation of IPS activity. Thus, this study aimed at investigating whether
110 numerosity estimations of self-generated words were attenuated compared to numerosity
111 estimations of passively heard words, thereby demonstrating that self-attenuation applies
112 to cognitive processes beyond sensory processing.

113 To investigate which brain regions and networks showed activity related to attenuation
114 processes, we designed a functional magnetic resonance imaging (fMRI) paradigm allowing
115 the controlled comparison of numerosity estimations of either self-generated words (active
116 condition) during a phonetic verbal fluency task or externally-generated words (passive
117 condition) while passively listening to a stream of words. Additionally, we asked participants
118 to evaluate the error they could have made in their estimation (performance monitoring).
119 Assuming that attenuation occurs during numerosity estimations (active condition), we

120 predicted that participants would underestimate the number of self- vs. externally-
121 generated words and explored possible effects on performance monitoring. As performance
122 monitoring is better for self-initiated vs. observed processes (Pereira et al., 2020), we
123 expected to find a stronger relationship between the reported and actual number of words
124 in the active vs. passive condition. At the neural level, considering that sensory attenuation
125 of self-generated stimuli involves the corresponding sensory brain regions (e.g., primary
126 auditory cortex for attenuated sounds, see Rummell et al., 2016; Whitford, 2019), we
127 expected to find reduced BOLD signal during the active vs. passive condition in areas
128 responsible for numerosity processing including the IPS.

129 **METHODS**

130 **Participants**

131 Three independent participant groups were tested in this study. First, we performed a
132 behavioral pilot experiment in a mock scanner, where we tested 17 (6 women) participants
133 (age range: 18 – 28 years; M = 23 years, CI(95%) = [23, 24]); schooling level varied between
134 13 and 21 years; M = 17 years, CI(95%) = [16, 18]). During the main fMRI experiment, we
135 studied 25 (14 women) participants (age range: 18 – 37 years; M = 23 years, CI(95%) = [22,
136 26]; schooling level varied from 12 to 22 years: M = 17 years, CI(95%) = [16, 18]). An
137 additional control experiment in the mock scanner was performed, where 14 (12 women)
138 participants were tested (age range: 18 – 29 years; M = 24 years, CI(95%) = [22, 26]);
139 schooling level varied between 10 and 23 years; M = 16 years, CI(95%) = [14, 18]). All
140 participants were right-handed according to the Edinburgh Hand Preference Inventory
141 (Oldfield, 1971) and native French-speaking healthy volunteers with no history of
142 neurological or psychiatric disease and no recent reported history of drug use. Participants
143 had normal or corrected-to-normal vision and no claustrophobia. All participants were naive
144 to the purpose of the study, gave informed consent in accordance with institutional
145 guidelines and the Declaration of Helsinki, and received monetary compensation (20 CHF /
146 hour). The study was approved by the local ethical committee of the canton Geneva
147 (protocol ID: 2015-00092).

148 **Experimental task**

149 The experiment was performed in a mock scanner environment (both for the behavioral
150 pilot experiment and the training for the main fMRI experiment) and in the MRI scanner

(main fMRI experiment). The task consisted in phonetic verbal fluency and passive word listening parts, followed by numerosity and error estimations (Figure 1). The task comprised two conditions (20 trials each) during which participants either covertly generated words (active condition) or listened to pre-recorded words (passive condition). Each trial started with a randomly jittered inter-trial interval varying between 4 s and 4.75 s, followed by an audio cue (2 s) indicating which of the active or passive condition will follow, and a recorded cue letter (2 s). Next, the word generation phase lasted between 20 s and 35 s; in the active condition, participants had to covertly generate words starting with the cued letter (Figure 1, top). For each word they covertly generated, participants were asked to press a response button, which gave us access to the actual number of generated words. In the passive condition, a series of pre-recorded audio words were played to the participants, who were asked to press the response button for every word that contained the cue letter (Figure 1, bottom). We avoided asking participants to detect words starting with the cued letter, as this could have influenced word generation in the next active trials with the same cued letter. In both conditions, the end of the generation/listening phase was indicated by an audio cue (0.5 s). After that, participants first reported the estimation of a total number of words generated (active condition) or heard (passive condition). For this, they used two buttons that moved a slider displayed on the screen. The slider was presented as a random integer (ranging from 0 to 20), which could be changed in value by pressing the response box buttons (left button – decrease the value, right button – increase the value). This was followed by an error estimation, where participants were asked to evaluate their performance on the numerosity estimation by estimating the magnitude of the error they thought they might have made (in number of words). For this, an automatically sliding bar was presented, and the participant had to select with one button press the desired value

175 (e.g., +/- 2 words error). Values varied from +/- 0 words (e.g., numerosity response judged
 176 as correct) to +/- 5 words mistaken. The total time for numerosity and error estimations
 177 were restricted to a maximum of 7 s. Except for the numerosity and error estimation
 178 periods, participants were asked to perform the task with eyes closed.

179

180 **Stimuli**

181 All stimuli were prepared and presented using Matlab 2016b (mathworks.com) and the
 182 Psychtoolbox-3 toolbox (psychtoolbox.org; Brainard 1997; Kleiner et al. 2007; Pelli 1997).
 183 Twenty different cue letters were used for active and passive conditions. The same cue
 184 letter was used once during the active and once during the passive condition in the
 185 counterbalanced order. Played back words during the passive condition were chosen from a
 186 list of 420 French words (Ferrand and Alario, 1998). The audio stimuli presented during the
 187 task were recorded by male and female native French speakers in a neutral manner and
 188 registered in *wav* format with 11025Hz sampling frequency. The gender of the voice
 189 pronouncing words in the passive condition was matched to the participants' gender. During
 190 the experiment, participants were equipped with MRI compatible earphones and report
 191 buttons for the right hand.

192 **Procedure**

193 Participants were trained in a mock scanner prior to the main fMRI experiment in order to
 194 familiarize themselves with the task. They were asked to perform four trials of the task
 195 during the training (twice for each condition), with the cue letters 'j' and 'k'. These letters
 196 were not used later during the main fMRI experiment. We note that participants were

197 instructed by the experimenter not to count nor use any strategy to try to remember the
198 number of words generated/heard while performing numerosity and error estimations.

199 The main experiment consisted of three runs lasting approximately 15 min, each with short
200 breaks in-between. The total duration of a trial varied between 40 and 55 s due to
201 pseudorandomized time for the word generation/ listening phase. This time variability was
202 introduced to avoid habituation and predictability for the number of generated/heard
203 words and to decorrelate hemodynamic activity related to word generation/listening and
204 numerosity estimations. The experiment was designed in 10 blocks with 4 trials of the same
205 condition per block. The blocks of the active condition trials always preceded the blocks of
206 the passive condition, allowing us to use the number and pace of generated words that
207 were recorded based on participant's button presses to playback the words during the next
208 block of the passive condition. The order of the number of words played with their
209 corresponding pace during the passive condition was shuffled within the block. This was
210 done to ensure that participants could not recognize whether the number and pace of the
211 played words matched the preceding active condition block. Additionally, to avoid repetition
212 effects between blocks, the cue letters between two consecutive blocks were different,
213 meaning that the cue letters in a given active block were not used in the following passive
214 block.

215 After the main experiment, a standard phonemic verbal fluency (generation time of 60 s,
216 cue letter 'p') test (Lezak, 1995) was performed overtly to verify that subjects understood
217 the task correctly. Overall, the experiment lasted approximately 1h 30 min (MRI session)
218 and 1h in the mock scanner (pilot session). The pilot mock scanner study contained the

219 same procedure as the main MRI experiment, except for the shorter breaks between the
 220 runs since there was no scanning involved.

221 The sample size for the main fMRI experiment was based on a recent study from our group
 222 in which similar conditions were contrasted (e.g., judgement of self-generated vs. observed
 223 decisions; Pereira et al., 2020).

224 **Control order experiment**

225 An additional control experiment in the mock scanner was performed to rule out the
 226 possibility that repetition effects occurred between consecutive blocks. It consisted only of
 227 passive condition trials, which were divided into ‘random’ and ‘repeated’ blocks. The
 228 ‘random’ block trials were designed by pseudo-randomly generating the number of words
 229 played (mean of 10 words/block ranging from 6 to 20 words per trial) and their playing pace
 230 (total time of playing varied between 20 s and 35 s) to match the main fMRI experiment.
 231 ‘Repeated’ blocks consequently followed ‘random’ blocks, with the same number of words
 232 and word playing pace as in the preceding random block but with a shuffled order. This
 233 control experiment consisted of 2 ‘random’ and 2 ‘repeated’ blocks, with 4 trials/block, and
 234 lasted approximately 30 min.

235

236 **Behavioral performance measures**

237 Most statistical frameworks to analyze performance monitoring have been developed for
 238 discrimination tasks with a binary response (e.g., Fleming and Lau, 2014 for a review). In the
 239 following, we propose two indices of numerosity performance and performance monitoring
 240 to analyze ordinal data (e.g., number of words). In addition to the prerequisites described

241 below, these indices were defined at the single-trial level so they could serve as parametric
 242 regressors of interest in the fMRI analysis.

243 The numerosity performance index is a normalised accuracy ratio reflecting how correctly
 244 participants estimated the number of words during the generation/listening phase. For each
 245 trial, we wanted signed numerosity performance to be proportional to the difference
 246 between the reported number of generated/heard words (numerosity estimation; [N]) and
 247 the actual number of words generated/heard [W]. We normalized this difference by the
 248 sum of numerosity estimation and actually generated/heard number of words [N+W]
 249 (equation 1) to give more weight to errors made about low numbers of words (e.g., an error
 250 of +/- 2 given a numerosity estimation of 8 has higher magnitude than an error of +/-2 given
 251 a numerosity estimation of 16; Figure 1-1 A). This normalization allowed us to assess
 252 attenuation effects independent of the number of generated words, given that the precision
 253 of numerosity estimation linearly decreases with increasing number of items (e.g., Piazza et
 254 al., 2004). Negative numerosity performance values thus reflected an underestimation of
 255 generated/heard words, and positive values reflected an overestimation of
 256 generated/heard words. In contrast, null numerosity performance values reflected correct
 257 answers about the number of generated/heard words.

$$258 \text{ numerosity performance} = \frac{N - W}{N + W} \text{ (equation 1)}$$

259

260 Additionally to the numerosity performance index, we derived separate measures of
 261 accuracy [N-W] and accuracy ratio [(N-W)/W] to assess the generalizability of our findings.

262 Performance monitoring reflected how well participants estimated an error about their
 263 previous performance. We defined it as the absolute value of the difference between the
 264 error estimation [E] and (accuracy [N-W]), normalized by the sum of the numerosity
 265 estimation and words generated/heard [N+W]) (equation 2). Normalization was done in
 266 order to consider the difficulty; the same error made when estimating the low number of
 267 words or high number of words should be penalized proportionally. A performance
 268 monitoring value of 0 reflected ideal error tracking, whereby participants correctly
 269 estimated the error made during the numerosity estimation. An increase in performance
 270 monitoring value represented an increase in error magnitude while estimating the
 271 difference between numerosity estimation and the actual number of words
 272 generated/heard (Figure 1-1 B).

$$273 \text{ performance monitoring} = \left| \frac{E - |N - W|}{N + W} \right| \text{ (equation 2)}$$

274

275 Data cleaning was performed prior to statistical analysis: trials for which participants did not
 276 generate at least five words or failed to answer numerosity or error estimations within the
 277 time limit were excluded from behavioral and fMRI analysis (in total, 2.44 ± 1.87
 278 trials/subject were excluded). The threshold of 5 words was selected according to the
 279 working memory capacity of 5 ± 2 items (Cowan, 2010). Considering all participants' data,
 280 6.1% of all trials were discarded.

281 **Behavioral data analysis**

282 All continuous variables (numerosity performance, accuracy, accuracy ratio and
 283 performance monitoring) were analyzed using linear mixed-effects regressions with

condition ("active", "passive" or "random", "repeat" for the control order experiment) as a fixed effect and a random intercept by participant and condition. The inclusion of additional random effects was guided by model comparison and selection based on Bayesian Information Criteria. Analyses were performed using the lme4 (Bates et al., 2015) and lmerTest (Kuznetsova et al., 2017) packages in R (R-project.org). The significance of fixed effects was estimated using Satterthwaite's approximation for degrees of freedom of F statistics (Luke, 2017).

Bayesian analysis was performed using the brms package (Bürkner, 2017) in R to examine the occurrence of possible repetition effects between random and repeated passive blocks in the control experiment. Namely, we conducted a Bayesian linear model of numerosity performance with condition ("random", "repeated") as fixed effects and a random intercept by participant and condition with four chains of 10000 iterations including 2000 warmup samples. We made a prior assumption that underestimation would be observed in the passive condition (prior with Gaussian distribution of mean = -0.032 and SD = 0.156), based on the difference between numerosity performance during the active and passive conditions observed in the main fMRI experiment.

Data simulation of absolute accuracy during numerosity estimations

To examine whether absolute accuracy (correct numerosity estimations of words generated/heard) of numerosity estimations observed in the experimental data may be approximated by a noisy sampling process rather than counting, we performed data simulations. More specifically, we simulated 1000 numerosity estimations (as the main experiment contained 40 trials/subject * 25 subjects) from a normal distribution centred on 10 and standard deviation (SD) varying from 0.5 to 6 with 0.1 steps. We rounded each item

307 to the nearest integer and counted how many times the number 10 was obtained. The
 308 simulation was iterated 10000 times.

309 **fMRI data acquisition**

310 MRI data were acquired using a Siemens Magnetom Prisma 3 T scanner with a 64-channel
 311 head coil. T1 weighted (1 mm isotropic) scans were acquired using a Magnetization
 312 Prepared Rapid Acquisition Gradient Echo (MPRAGE) sequence (TR = 2300 ms; TI = 900 ms;
 313 TE = 2.25 ms; flip-angle = 8 degrees; GRAPPA = 2; FOV = 256 × 256 mm; 208 slices).
 314 Functional scans were obtained using echo-planar (EPI) sequence (multiband acceleration =
 315 6; TR = 1000 ms; TE = 32 ms; flip-angle = 58 degrees; FOV = 224 × 224 mm; matrix = 64 × 64;
 316 slice thickness = 2 mm; number of slices = 66). The number of functional image volumes
 317 varied according to the experiment duration (2278 ± 61 volumes).

318 **fMRI data preprocessing**

319 Anatomical and functional images were processed and analyzed using SPM-12 (Wellcome
 320 Centre for Human Neuroimaging, London, UK). Pre-processing steps included slice time
 321 correction, field-map distortion correction, realignment and unwarping to spatially correct
 322 for head motions and distortions, co-registration of structural and functional images,
 323 normalization of all images to common Montreal Neurological Institute (MNI) space, and
 324 spatial smoothing with a Gaussian kernel with a full-width at half maximum (FWHM) of 4
 325 mm. Quality assurance of all EPI images was performed with the criteria of maximum 2 mm
 326 translation and 2° rotation between volumes. In addition, an excessive movement was
 327 estimated with the mean framewise displacement (FD) (Power et al., 2012) with the
 328 exclusion threshold of 0.5 mm. None of the subjects had a higher mean FD (0.2 ± 0.06 mm)
 329 than the set threshold.

330 **fMRI data analysis**

331 We used a two-level random-effects analysis. In the first-level analysis, condition-specific
332 effects were estimated according to a general linear model (GLM) fitted for each subject. An
333 average mask of grey matter from all subjects was built using FSL (fsl.fmrib.ox.ac.uk/fsl) and
334 used to mask out white matter and non-brain tissues. The GLM was built using six boxcar
335 regressors corresponding to the duration of the word generation/listening phase,
336 numerosity estimation and error estimation in the active and passive conditions. Parametric
337 modulators of numerosity performance and performance monitoring were included in the
338 numerosity estimation and error estimation regressors, respectively. Further, we added
339 regressors of no interest corresponding to audio instructions, button presses and excluded
340 trials, plus six regressors for head motion (translation and rotation).

341 At the second-level (group level), we performed a one-way analysis of variance (ANOVA)
342 with F-tests to assess main effects common to active and passive conditions and t-tests to
343 analyze the difference between conditions (active vs. passive) for each regressor of interest:
344 numerosity estimation and error estimation. We used a voxel-level statistical threshold of
345 $p < 0.001$ and corrected for multiple comparisons at the cluster level using family-wise error
346 (FWE) correction with the threshold of $p < 0.05$. We used the anatomical automatic labelling
347 (AAL) atlas for brain parcellation (Tzourio-Mazoyer et al., 2002).

348 **Functional connectivity analysis**

349 Psychophysiological Interaction (PPI) analysis was employed to identify modulations of
350 functional coupling between a seed region and other brain regions by experimental
351 conditions (active vs. passive) (Friston et al., 1997). To perform this analysis we used

generalized psychophysiological interaction (gPPI) toolbox version 13.1 (McLaren et al., 2012). Spheres of 6 mm radius were formed around the peak coordinates of the right IPS ($x = 29$; $y = -65$; $z = 50$) and the left IPS ($x = -27$; $y = -66$; $z = 47$) clusters that were identified in the second-level analyses. First-level (individual) GLM analyses were performed, including task regressors of numerosity estimation or error estimation (psychological term) and time course of the seed region (physiological term). As for other aforementioned fMRI analyses, we performed t-tests to compare the differences between conditions.

Data and code availability

The MRI data that support the findings of this study is available on a public repository on zenodo.org (<https://doi.org/10.5281/zenodo.4925909>). Behavioral data, analysis and task codes are available here: <https://gitlab.epfl.ch/Inco-public/cognitive-attenuation>.

RESULTS

Behavioral results

By design, the number of generated and heard words was matched between conditions (active: $M = 10.7$, $SD = 3.6$, $CI(95\%) = [10.4, 11.1]$; passive: $M = 10.7$, $SD = 3.5$, $CI(95\%) = [10.4, 11.0]$, $F_{(1,884)} = 0.005$, $p = 0.94$). The duration of word generation and listening did not differ between conditions either (active: $M = 27.4$, $SD = 5.6$, $CI(95\%) = [26.9, 27.9]$; passive: $M = 28.4$, $SD = 7.0$, $CI(95\%) = [27.7, 29.0]$, $F_{(1,26)} = 2.04$, $p = 0.16$). Having shown that conditions were similar in terms of difficulty, we turned to the analysis of numerosity performance and performance monitoring.

Numerosity performance indices revealed that globally, participants underestimated the number of words ($M = -0.05$, $SD = 0.11$, $CI(95\%) = [-0.06, -0.05]$). This underestimation was

significantly larger ($F_{(1,24)} = 5.85$, $p = 0.023$, 18 subjects out of 25 showed the effect) in the active condition ($M = -0.07$, $SD = 0.11$, $CI(95\%) = [-0.08, -0.06]$) compared to the passive condition ($M = -0.04$, $SD = 0.12$, $CI(95\%) = [-0.05, -0.03]$) (Figure 2 A). Comparable results were obtained during the pilot experiment in the mock scanner in an independent group of subjects (active: $M = -0.05$, $SD = 0.01$, $CI(95\%) = [-0.06, -0.03]$); passive: $M = -0.03$, $SD = 0.10$, $CI(95\%) = [-0.04, -0.02]$; $F_{(1,16)} = 5.80$ $p = 0.016$). These two experiments suggest that numerosity estimations for self-generated words are attenuated.

We further show that the larger underestimation in the active compared to the passive condition was also found when considering the measures of accuracy (active: $M = -1.48$, $SD = 2.38$, $CI(95\%) = [-1.69, -1.26]$); passive: $M = -0.94$, $SD = 2.59$, $CI(95\%) = [-1.17, -0.71]$; $F_{(1,24)} = 4.43$ $p = 0.045$) and accuracy ratio as dependent variables (active: $M = 0.89$, $SD = 0.20$, $CI(95\%) = [0.87, 0.91]$); passive: $M = 0.95$, $SD = 0.23$, $CI(95\%) = [0.93, 0.97]$; $F_{(1,24)} = 7.44$ $p = 0.011$).

We then assessed the linear relationship between the reported (numerosity estimation) and actual number of words (Figure 2 B). Besides a main effect of words ($F_{(1,908)} = 1042$, $p < 0.001$) and of condition ($F_{(1,198)} = 8.25$, $p = 0.0045$), we found an interaction between condition and generated/heard words ($F_{(1,802)} = 4.3$, $p = 0.038$). This interaction was driven by a steeper slope in the active condition ($M = 0.62$, $CI(95\%) = [0.57, 0.67]$) compared to the passive condition ($M = 0.55$, $CI(95\%) = [0.50, 0.60]$) (Figure 2 C), which indicates better numerosity tracking for self-generated words during the main fMRI experiment (a slope of value 1 reflecting ideal performance). We note that this interaction did not reach significance in our pilot experiment ($F_{(1,350)} = 1.10$, $p = 0.66$), which calls for interpreting this result with caution.

397 Next, we investigated whether performance monitoring varied between conditions, by
 398 quantifying how well participants were able to track the error made when estimating the
 399 number of generated/heard words. We found no differences in performance monitoring
 400 ($F_{(1,24)} = 1.09$, $p = 0.3$) between the active ($M = 0.07$, $SD = 0.06$, $CI(95\%) = [0.07, 0.08]$) and
 401 passive ($M = 0.08$, $SD = 0.06$, $CI(95\%) = [0.07, 0.09]$) conditions during the main fMRI
 402 experiment, nor during the mock scanner pilot experiment ($F_{(1,16)} = 0.78$, $p = 0.39$; active: M
 403 $= 0.07$, $SD = 0.06$, $CI(95\%) = [0.06, 0.08]$; passive: $M = 0.06$, $SD = 0.06$, $CI(95\%) = [0.06, 0.07]$).
 404 This confirms the absence of evidence supporting an effect of attenuation on performance
 405 monitoring.

406 Finally, we carried out a control task for word generation outside the scanner, during which
 407 participants had to perform a standard verbal fluency task overtly with the cue letter 'p'.
 408 Comparing the number of words generated, starting with the letter 'p' overtly (outside the
 409 scanner) and covertly (during the scanning), we did not observe any significant differences
 410 between the number of words generated overtly ($M = 12.6$, $SD = 3.79$, $CI(95\%) = [10.9,$
 411 $14.1]$) and covertly ($M = 12.3$, $SD = 3.96$, $CI(95\%) = [10.6, 13.9]$; paired t-test; $t_{(24)} = -0.4$;
 412 $p = 0.69$). This control task confirms that subjects did generate words covertly and
 413 comparably to overt fluency, as instructed.

414 *Control order experiment.* The global underestimation ($M = -0.06$, $SD = 0.11$, $CI(95\%) = [-$
 415 $0.08, -0.05]$) was replicated as in the main experiment. This underestimation was not
 416 different ($F(1,117) = 0.03$, $p = 0.87$) between 'random' ($M = -0.06$, $SD = 0.12$, $CI(95\%) = [-$
 417 $0.09, -0.04]$) and 'repeated' ($M = -0.07$, $SD = 0.12$, $CI(95\%) = [-0.09, -0.04]$) blocks, with a
 418 Bayes factor $BF_{10} = 0.09$ supporting the absence of difference between conditions.

419 *Data simulation of absolute accuracy during numerosity estimations.* As can be seen on the
 420 Figure 3, the value of 10 occurred in 19.5% of all data points when drawn from a normal
 421 distribution with SD = 2, similarly to the observed empirical data.

422

423 **fMRI results**

424 **Numerosity performance**

425 Brain activity during the numerosity estimation phase was widespread, irrespective of the
 426 experimental condition (Table 1-1). Differences between conditions revealed widespread
 427 relative deactivations in the active compared to the passive condition in the bilateral
 428 parietal cortex including IPS, middle-superior temporal gyri, precuneus, cerebellum, middle
 429 cingulate gyri, SMA, insula, middle-superior frontal gyri, hippocampus, caudate nucleus,
 430 putamen (for the detailed list of all areas see Table 1).

431 To avoid contaminating the results with inherent differences between the active and passive
 432 conditions that are not specific to numerosity processes, we looked for brain activity
 433 parametrically modulated by numerosity performance. We found a single brain region with
 434 such a pattern of activity, namely the right IPS, whose activity was negatively correlated
 435 with numerosity performance (main effect $F = 20.0$, $p_{FWE} = 0.042$, $k_{vox} = 148$, $x = 29$, $y = -65$, z
 436 $= 50$; Figure 4 A, B). The same pattern was found bilaterally when using a less stringent
 437 threshold ($p < 0.005$ peak level uncorrected; Figure 4 C, Table 2). Unlike our prediction, IPS
 438 activation did not differ between the active and passive conditions ($p_{FWE} > 0.05$), suggesting
 439 that this effect was independent of whether words were heard or actively generated.

440 Using PPI analysis, we investigated whether the functional connectivity of the right IPS with
 441 other brain regions differed between the active and passive conditions. This analysis
 442 revealed that bilateral supplementary motor area (SMA), left inferior parietal lobule (IPL)
 443 and left superior temporal gyrus (STG) had increased connectivity with the right IPS in the
 444 active compared to the passive condition (Figure 5, Table 3). No effect in the other direction
 445 was observed.

446

447 **Performance monitoring**

448 Besides numerosity performance, we also quantified brain activity during the error
 449 estimation phase. We found widespread cortical and subcortical activations during this
 450 phase compared to baseline, irrespective of the experimental condition (Table 4-1).
 451 Moreover, bilateral insula and right putamen were significantly less active during the active
 452 compared to the passive condition (Figure 6, Table 4). The left caudate nucleus showed the
 453 opposite pattern, with higher activity in the passive than in the active condition.

454 To avoid confounding factors between the active and passive condition, we looked more
 455 specifically at parametric modulations of error monitoring. We observed that BOLD signal in
 456 the left IPS was more related to performance monitoring in the active compared to the
 457 passive condition ($t = 4.02$, $p_{FWE} = 0.041$, $k_{vox} = 198$, $x = -27$, $y = -66$, $z = 47$; Figure 7).
 458 Interestingly, this activation cluster spatially overlapped with the observed activation cluster
 459 related to the main effect of numerosity performance when applying a lower statistical
 460 threshold (exploratory analysis, $p < 0.005$ peak level uncorrected, $p_{FWE} < 0.05$ cluster level)
 461 (see Figure 4 C).

462 Lastly, results from the PPI analysis using the left IPS as a seed ROI did not reveal any
463 functional connectivity differences between the active and passive conditions during error
464 estimation.

465

466

467 **DISCUSSION**

468 The present study examined whether attenuation of self-generated stimuli impacts
 469 cognitive processes beyond the traditionally investigated sensory processes, namely
 470 numerosity estimations and performance monitoring. To this end, we developed an
 471 experimental paradigm allowing the controlled comparison of numerosity estimations and
 472 performance monitoring regarding self- and externally-generated words while acquiring
 473 fMRI data. We found that participants more strongly underestimated the number of self-
 474 compared to externally-generated words, providing behavioral evidence that numerosity
 475 estimations are indeed subject to attenuation. As expected, numerosity performance was
 476 associated with hemodynamic activity changes in IPS. Furthermore, a network including the
 477 bilateral SMA, left IPL and left STG showed increased functional connectivity with the right
 478 IPS during numerosity estimations for self-generated words, suggesting that numerosity-
 479 related attenuation involves this neural network. Finally, by asking participants to monitor
 480 the accuracy of their own numerosity estimations, we found equivalent performance
 481 monitoring for self- and externally-generated words. Although no difference was found at
 482 the behavioral level, we found that performance monitoring was associated with increased
 483 IPS activity in the active vs. passive condition.

484 **Behavioral and neural markers of attenuated numerosity estimations**

485 Participants underestimated the number of words they generated or heard. Such
 486 underestimations were previously described regarding the numeric estimation of perceptual
 487 quantities (e.g., number of dots or sequences of sounds) to discrete measures (e.g., Arabic
 488 numeral) (Castronovo and Seron, 2007; Reinert et al., 2019). In the present study, we found
 489 that word numerosity underestimation was stronger in the active compared to the passive

490 condition, in line with our hypothesis that attenuation of self-generated stimuli may extend
 491 to higher-level cognitive functions (Kilteni et al., 2018; Jack et al., 2019). Of note, this
 492 underestimation could not be due to simple repetition effects between successive blocks of
 493 active and passive condition trials, as a control experiment showed no differences in
 494 numerosity estimations between repeated blocks of passive condition trials.

495

496 Attenuation of self-generated stimuli has been mostly investigated for sensory processes
 497 and refers to the diminished behavioral and neural responses associated with self-
 498 generated compared to externally-generated stimuli (Timm et al., 2014; Benazet et al.,
 499 2016). Importantly, attenuation has recently also been described for imagined actions in the
 500 absence of overt actions (e.g., Kilteni et al., 2018; Jack et al., 2019;). For example, imagined
 501 self-touch was felt as less intense compared to externally applied touch (Kilteni et al., 2018).
 502 Similarly, imagined speech elicited reduced electrophysiological signals related to auditory
 503 processing (Whitford et al., 2017). These studies, however, investigated cognitive processes
 504 intimately linked to sensorimotor systems (e.g., imagined movement and touch), yet, to the
 505 best of our knowledge, it was unknown whether comparable mechanisms of attenuation
 506 also affect cognition beyond sensorimotor processing, such as numerosity estimations with
 507 no or less obviously implicated sensorimotor processes (e.g., Dehaene, 1997). Here we show
 508 that differential attenuation can be observed for cognitive processes such as numerosity
 509 estimations that depend on whether they are self-generated or not. As of today, there is no
 510 consensus to explain how the brain attenuates expected (e.g., self-generated) stimuli while
 511 remaining sensitive to unexpected ones (for a recent review and unifying theoretical
 512 account see Press et al., 2020). Among the so-called cancellation theories, the internal

513 forward model (Farrer and Frith, 2002; Miall and Wolpert, 1996) proposes that corollary
514 discharges related to action are used to predict the sensory consequences of that action.
515 When such predictions match the actual sensory feedback from the action, its sensory
516 consequences are attenuated, and the action is perceived as self-generated (Wolpert and
517 Flanagan, 2001). The forward model thus proposes to link sensory attenuation to the
518 sensory predictions generated by a neural comparator. An analogous mechanism has been
519 proposed to account for attenuation for covert actions such as motor imagery (Kilteni et al.,
520 2018) or inner speech (Tian and Poeppel, 2010). The present data show that attenuation
521 exists beyond overt and covert actions, raising the possibility that the forward model
522 extends to repetitive cognitive activity (e.g., fluency and related numerosity estimations).
523 One possibility, similar to what has been described for inner speech, would be that
524 numerosity underestimation stems from a weaker perceptual representation of self-
525 generated words. In other words, attenuation may not impact numerosity estimations
526 directly, but rather through a decreased representation of self-generated words, which in
527 turn may lead to attenuation of numerosity estimations.

528 A second account could be that mental operations have a gating effect (Cromwell et al.,
529 2008), independent from predictive mechanisms, thereby directly affecting the strength of
530 the mental representations of self-generated words. A similar gating mechanism has
531 recently been shown to offer a plausible alternative to forward model accounts of sensory
532 self-attenuation (Thomas et al., 2020). Finally, the general mechanisms put forward by the
533 predictive coding account of active inference to explain sensory attenuation may also apply
534 to non-perceptual cognitive attenuation such as the one we observed (Brown et al., 2013).

535 At the neural level, the IPS showed activity related to numerosity performance, in line with
536 previous studies (Cohen and Dehaene, 1996; Piazza et al., 2006). This relation, however, was
537 not modulated by condition (active vs. passive), as one could have expected based on
538 previous reports showing that sensory attenuation coincides with decreased activity in the
539 corresponding sensory area (e.g., attenuation in primary auditory cortex during self-
540 generated auditory stimuli; Rummell et al., 2016; Whitford, 2019). Importantly, we found
541 differences in functional coupling during numerosity estimations of the IPS with a network
542 of brain regions between the active and passive conditions. The increase in coupling during
543 the active condition occurred between the IPS and a network comprising the SMA, IPL and
544 STG, known to be involved in predictive processing, for example of self-generated auditory
545 and imagery speech (Lima et al., 2016; Tian et al., 2016). Although previous neuroimaging
546 studies have mainly shown attenuated brain activity for self-generated actions (e.g.,
547 Whitford, 2019), increases in functional connectivity such as we describe have been
548 reported in the primary auditory cortex during attenuated speech (van de Ven et al., 2009),
549 or of somatosensory cortex during attenuated touch (Kilteni and Ehrsson, 2020). Thus,
550 increased functional connectivity in a network centred on the key numerosity region, IPS,
551 and that has been associated with speech-related processing further supports that
552 numerosity underestimation stems from a process related to attenuation when participants
553 self-generate words.

554

555 Besides numerosity underestimation, we observed that participants formed more accurate
556 numerosity judgments for self- vs. externally-generated words: while participants' word
557 estimations were lower in the active condition than in the passive condition, the relation

558 between their estimated number of words and the actual number of words was better in
 559 the active condition vs. passive condition, suggesting a sharper representation of the
 560 number of self-generated words. This result corroborates recent findings showing better
 561 monitoring for decisions that are committed rather than observed (Pereira et al., 2020). This
 562 improved monitoring of self-generated words could be related to the sharpening of
 563 expected representations known in the sensory domain (Kok et al., 2012) or to a self-
 564 generation effect underlying the facilitation of information encoding and enhanced recall for
 565 self-generated stimuli (Bertsch et al., 2007; Slamecka and Graf, 1978). We note that this
 566 effect was not replicated during the mock pilot experiment, which included a smaller
 567 sample of participants with a globally higher absolute accuracy. It is possible that this subtle
 568 effect could not be observed in such conditions, which warrants future investigations and
 569 cautious interpretation.

570 **Performance monitoring is modulated at the neural but not behavioral level**

571 Previous research has shown that both humans and non-human primates (Beran et al.,
 572 2006; Duyan and Balci, 2019, 2018) can monitor the quality of their numerosity estimations.
 573 Thus, in addition to asking participants to estimate the number of words they generated or
 574 heard, we also asked them to estimate their own error during this process (performance
 575 monitoring). Although our behavioral results showed similar performance monitoring
 576 between conditions, we observed that performance monitoring was associated with
 577 hemodynamic activity in the left IPS predominantly in the active condition. Interestingly, this
 578 region is not typically associated with performance monitoring such as the prefrontal cortex
 579 or the insula/inferior frontal gyrus (Vaccaro and Fleming, 2018). Since activity in the left IPS
 580 is related to numerosity estimation (Cappelletti et al., 2007; Dormal et al., 2012), this

parametric modulation could therefore represent a substrate for monitoring specific to numerosity estimations. By investigating global fMRI activity during error estimations, we also observed decreased activation in the insula and putamen and increased activity in the caudate nucleus when comparing the active vs. passive conditions. To note, the anterior insula and putamen were activated during both conditions but were attenuated in the active compared to the passive conditions. While the anterior insula activations are consistent with previous literature on performance monitoring (Ullsperger et al., 2010; Bastin et al., 2017), the findings of modulated activity in the striatum were unexpected. Both areas are known as essential for the control of goal-directed decision-making (Balleine et al., 2007; Kim and Im, 2019). Further links between performance monitoring and activity modulation between conditions in the striatum regions should be explored in future studies.

Methodological considerations

As generating vs. listening to words inherently involves different behavioral and neural processes, several aspects of our design should be considered when interpreting the current findings as reflecting attenuation per se rather than experimental confounds. At the behavioral level, the larger underestimation during the active condition was not due to difficulty differences between conditions as task difficulty was matched by design, and absolute accuracy (correct numerosity estimations of words generated/heard) was similar in both conditions. Of note, a steeper slope during numerosity estimations and number of words generated in the active condition suggests that participants better tracked their performance even when underestimating more compared to the passive condition. Although we could not explicitly control whether participants counted the number of words they generated or heard, instructions were given not to do so. Yet, counting seems unlikely

604 as absolute accuracy reached only 19.5% of all trials, which is comparable to a recent study
605 with a similar setup (Serino et al., 2021), and much lower than what is typically observed
606 when participants are instructed to count (e.g. Kansaku et al., 2007). Furthermore, a similar
607 level of absolute accuracy was obtained on simulated data with numerosity estimations
608 drawn from a normal distribution with $SD = 2$, suggesting that behavior in this task is
609 approximated by a noisy sampling process rather than counting. At the neural level, to
610 ensure that the inherent differences between conditions did not contaminate our results,
611 we focused analyses on the numerosity and error estimation phases which were identical
612 between conditions, instead of the word generation/listening phases. In addition, we did
613 not base our conclusions on a direct contrast between the two conditions, but on
614 correlations between neural activity and numerosity or error estimates.

615 **Conclusion**

616 Based on behavioral and neuroimaging data, we propose that higher-level cognitive
617 functions such as numerosity estimations about the number of self-generated words are
618 attenuated. Such attenuation involves a functional network including a key-numerosity
619 region (IPS) and speech-related regions including the SMA, IPL and STG. While attenuating
620 the sensory consequences of one's actions is of crucial importance for aspects of the self,
621 such as the sense of agency, attenuating the products of one's mental activities may also be
622 relevant to distinguish them from external sources of information. Our paradigm offers a
623 promising tool to investigate attenuation processes related to the self in cognition and to
624 compare and distinguish them from sensory attenuation processes. It may be of relevance
625 to the study of clinical cases in which attenuation in sensory and cognitive domains may be

626 is altered, including patients with psychotic symptoms like thought insertion whereby

627 thoughts are not considered as one's own, but of somebody else.

628

629 **Acknowledgments**

630 The authors are grateful for the technical support during data acquisition to the Foundation
631 Campus Biotech Geneva (FCBG) Human Neuroscience Platform of the Campus Biotech. This
632 work was supported by the Bertarelli Foundation (grant number 532024), the Swiss National
633 Science Foundation (grant number 3100A0-112493), National Center of Competence in
634 Research (NCCR) "Synapsy - The Synaptic Bases of Mental Diseases" (grant number 51NF40
635 – 185897), and two generous donors advised by Carigest SA. Nathan Faivre has received
636 funding from the European Research Council (ERC) under the European Union Horizon 2020
637 research and innovation programme (grant number 803122).

638

639 **Author Contributions**

640 GS, NF, GR, OB developed the study concept and contributed to the study design. Testing,
641 data collection and data analysis were performed by GS. GS, MP, JP and NF provided
642 methodological support. GS, NF, MP, and OB drafted the paper; all authors provided critical
643 revisions and approved the final version of the paper for submission.

644

645

646 **REFERENCES**

- 647 Anobile, G., Cicchini, G.M., Burr, D.C., 2016. Number As a Primary Perceptual Attribute: A
648 Review. *Perception* 45, 5–31. <https://doi.org/10.1177/0301006615602599>
- 649 Arsalidou, M., Taylor, M.J., 2011. Is 2+2=4? Meta-analyses of brain areas needed for
650 numbers and calculations. *Neuroimage* 54, 2382–2393.
651 <https://doi.org/10.1016/j.neuroimage.2010.10.009>
- 652 Baess, P., Horváth, J., Jacobsen, T., Schröger, E., 2011. Selective suppression of self-initiated
653 sounds in an auditory stream: An ERP study. *Psychophysiology* 48, 1276–1283.
654 <https://doi.org/10.1111/j.1469-8986.2011.01196.x>
- 655 Balleine, B.W., Delgado, M.R., Hikosaka, O., 2007. The role of the dorsal striatum in reward
656 and decision-making. *J. Neurosci.* 27, 8161–8165.
657 <https://doi.org/10.1523/JNEUROSCI.1554-07.2007>
- 658 Bansal, S., Ford, J.M., Sperling, M., 2018. The function and failure of sensory predictions.
659 *Ann. N. Y. Acad. Sci.* 1426, 199–220. <https://doi.org/10.1111/nyas.13686>
- 660 Bastin, J., Deman, P., David, O., Gueguen, M., Benis, D., Minotti, L., Hoffman, D.,
661 Combrisson, E., Kujala, J., Perrone-Bertolotti, M., Kahane, P., Lachaux, J.P., Jerbi, K.,
662 2017. Direct Recordings from Human Anterior Insula Reveal its Leading Role within the
663 Error-Monitoring Network. *Cereb. Cortex* 27, 1545–1557.
664 <https://doi.org/10.1093/cercor/bhv352>
- 665 Bates, D., Mächler, M., Bolker, B., Walker, S., 2015. Fitting Linear Mixed-Effects Models
666 Using lme4 | Bates | Journal of Statistical Software. *J. Stat. Softw.* 67.
- 667 Benazet, M., Thénault, F., Whittingstall, K., Bernier, P.M., 2016. Attenuation of visual

- 668 reafferent signals in the parietal cortex during voluntary movement. *J. Neurophysiol.*
 669 116, 1831–1839. <https://doi.org/10.1152/jn.00231.2016>
- 670 Beran, M.J., Smith, J.D., Redford, J.S., Washburn, D.A., 2006. Rhesus macaques (*Macaca*
 671 *mulatto*) monitor uncertainty during numerosity judgments. *J. Exp. Psychol. Anim.*
 672 *Behav. Process.* 32, 111–119. <https://doi.org/10.1037/0097-7403.32.2.111>
- 673 Bertsch, S., Pesta, B.J., Wiscott, R., McDaniel, M.A., 2007. The generation effect: A meta-
 674 analytic review. *Mem. Cogn.* 35, 201–210. <https://doi.org/10.3758/BF03193441>
- 675 Brainard, D.H., 1997. The Psychophysics Toolbox. *Spat. Vis.* 10, 433–436.
 676 <https://doi.org/10.1163/156856897X00357>
- 677 Brooks, J.X., Cullen, K.E., 2019. Predictive Sensing: The Role of Motor Signals in Sensory
 678 Processing. *Biol. Psychiatry Cogn. Neurosci. Neuroimaging* 4, 842–850.
 679 <https://doi.org/10.1016/j.bpsc.2019.06.003>
- 680 Brown, H., Adams, R.A., Parees, I., Edwards, M., Friston, K., 2013. Active inference, sensory
 681 attenuation and illusions. *Cogn. Process.* 14, 411–427. [https://doi.org/10.1007/s10339-](https://doi.org/10.1007/s10339-013-0571-3)
 682 013-0571-3
- 683 Bürkner, P.C., 2017. brms: An R package for Bayesian multilevel models using Stan. *J. Stat.*
 684 *Softw.* <https://doi.org/10.18637/jss.v080.i01>
- 685 Burr, D.C., Anobile, G., Arrighi, R., 2018. Psychophysical evidence for the number sense.
 686 *Philos. Trans. R. Soc. B Biol. Sci.* 373. <https://doi.org/10.1098/rstb.2017.0045>
- 687 Cappelletti, M., Barth, H., Fregni, F., Spelke, E.S., Pascual-Leone, A., 2007. rTMS over the
 688 intraparietal sulcus disrupts numerosity processing. *Exp. Brain Res.* 179, 631–642.

- 689 <https://doi.org/10.1007/s00221-006-0820-0>
- 690 Castronovo, J., Seron, X., 2007. Numerical Estimation in Blind Subjects: Evidence of the
 691 Impact of Blindness and Its Following Experience. *J. Exp. Psychol. Hum. Percept.*
 692 *Perform.* 33, 1089–1106. <https://doi.org/10.1037/0096-1523.33.5.1089>
- 693 Cohen, L., Dehaene, S., 1996. Cerebral Networks for Number Processing: Evidence from a
 694 Case of Posterior Callosal Lesion. *Neurocase* 2, 155–174.
 695 <https://doi.org/10.1080/13554799608402394>
- 696 Cowan, N., 2010. The magical mystery four: How is working memory capacity limited, and
 697 why? *Curr. Dir. Psychol. Sci.* 19, 51–57. <https://doi.org/10.1177/0963721409359277>
- 698 Cromwell, H.C., Mears, R.P., Wan, L., Boutros, N.N., 2008. Sensory gating: A translational
 699 effort from basic to clinical science. *Clin. EEG Neurosci.* 39, 69–72.
 700 <https://doi.org/10.1177/155005940803900209>
- 701 Dehaene, S., 1997. *The Number Sense*. Oxford Univ. Press.
- 702 DeWitt, I., Rauschecker, J.P., 2012. Phoneme and word recognition in the auditory ventral
 703 stream. *Proc. Natl. Acad. Sci. U. S. A.* 109, 505–514.
 704 <https://doi.org/10.1073/pnas.1113427109>
- 705 Dormal, V., Andres, M., Pesenti, M., 2012. Contribution of the right intraparietal sulcus to
 706 numerosity and length processing: An fMRI-guided TMS study. *Cortex* 48, 623–629.
 707 <https://doi.org/10.1016/j.cortex.2011.05.019>
- 708 Duyan, Y.A., Balci, F., 2019. Metric error monitoring in the numerical estimates. *Conscious.*
 709 *Cogn.* <https://doi.org/10.1016/j.concog.2018.11.011>

- 710 Duyan, Y.A., Balci, F., 2018. Numerical error monitoring. *Psychon. Bull. Rev.*
 711 <https://doi.org/10.3758/s13423-018-1506-x>
- 712 Farrer, C., Frith, C.D., 2002. Experiencing oneself vs another person as being the cause of an
 713 action: The neural correlates of the experience of agency. *Neuroimage* 15, 596–603.
 714 <https://doi.org/10.1006/nimg.2001.1009>
- 715 Ferrand, L., Alario, F.-X., 1998. Normes d'associations verbales pour 366 noms d'objets
 716 concrets. *Annee. Psychol.* 98, 659–709. <https://doi.org/10.3406/psy.1998.28564>
- 717 Fleming, S.M., Lau, H.C., 2014. How to measure metacognition. *Front. Hum. Neurosci.* 8, 1–
 718 9. <https://doi.org/10.3389/fnhum.2014.00443>
- 719 Friston, K.J., Buechel, C., Fink, G.R., Morris, J., Rolls, E., Dolan, R.J., 1997. Psychophysiological
 720 and modulatory interactions in neuroimaging. *Neuroimage* 6, 218–229.
 721 <https://doi.org/10.1006/nimg.1997.0291>
- 722 Hickok, G., 2012. Computational neuroanatomy of speech production. *Nat. Rev. Neurosci.*
 723 13, 135–145. <https://doi.org/10.1038/nrn3158>
- 724 Hughes, G., Waszak, F., 2011. ERP correlates of action effect prediction and visual sensory
 725 attenuation in voluntary action. *Neuroimage* 56, 1632–1640.
 726 <https://doi.org/10.1016/j.neuroimage.2011.02.057>
- 727 Jack, B.N., Le Pelley, M.E., Han, N., Harris, A.W.F., Spencer, K.M., Whitford, T.J., 2019. Inner
 728 speech is accompanied by a temporally-precise and content-specific corollary
 729 discharge. *Neuroimage* 198, 170–180.
 730 <https://doi.org/10.1016/j.neuroimage.2019.04.038>

- 731 Kansaku, K., Carver, B., Johnson, A., Matsuda, K., Sadato, N., Hallett, M., 2007. The role of
 732 the human ventral premotor cortex in counting successive stimuli. *Exp. Brain Res.* 178,
 733 339–350. <https://doi.org/10.1007/s00221-006-0736-8>
- 734 Kiltner, K., Andersson, B.J., Houborg, C., Ehrsson, H.H., 2018. Motor imagery involves
 735 predicting the sensory consequences of the imagined movement. *Nat. Commun.* 9, 1–
 736 9. <https://doi.org/10.1038/s41467-018-03989-0>
- 737 Kiltner, K., Ehrsson, H., 2020. Functional connectivity between the cerebellum and
 738 somatosensory areas implements the attenuation of self-generated touch. *J. Neurosci.*
 739 40, 894–906. <https://doi.org/10.1523/JNEUROSCI.1732-19.2019>
- 740 Kim, B.S., Im, H.I., 2019. The role of the dorsal striatum in choice impulsivity. *Ann. N. Y.*
 741 *Acad. Sci.* 1451, 92–111. <https://doi.org/10.1111/nyas.13961>
- 742 Kircher, T., David, A., 2003. *The Self in Neuroscience and Psychiatry, The self in neuroscience*
 743 *and psychiatry.* Cambridge University Press, Cambridge.
 744 <https://doi.org/10.1017/CBO9780511543708>
- 745 Kleiner, M., Brainard, D.H., Pelli, D.G., Broussard, C., Wolf, T., Niehorster, D., 2007. What's
 746 new in Psychtoolbox-3? *Perception* 36, S14. <https://doi.org/10.1068/v070821>
- 747 Kok, P., Jehee, J.F.M., de Lange, F.P., 2012. Less Is More: Expectation Sharpens
 748 Representations in the Primary Visual Cortex. *Neuron* 75, 265–270.
 749 <https://doi.org/10.1016/j.neuron.2012.04.034>
- 750 Kuznetsova, A., Brockhoff, P.B., Christensen, R.H.B., 2017. lmerTest Package: Tests in Linear
 751 Mixed Effects Models . *J. Stat. Softw.* 82. <https://doi.org/10.18637/jss.v082.i13>

- 752 Legrand, D., 2006. The bodily self: The sensori-motor roots of pre-reflective self-
 753 consciousness. *Phenomenol. Cogn. Sci.* 5, 89–118. [https://doi.org/10.1007/s11097-](https://doi.org/10.1007/s11097-005-9015-6)
 754 005-9015-6
- 755 Lezak, M.D., 1995. *Neuropsychological assessment* (3rd ed.), Neuropsychological
 756 assessment (3rd ed.).
- 757 Liebenthal, E., Binder, J.R., Spitzer, S.M., Possing, E.T., Medler, D.A., 2005. Neural substrates
 758 of phonemic perception. *Cereb. Cortex* 15, 1621–1631.
 759 <https://doi.org/10.1093/cercor/bhi040>
- 760 Lima, C.F., Krishnan, S., Scott, S.K., 2016. Roles of Supplementary Motor Areas in Auditory
 761 Processing and Auditory Imagery. *Trends Neurosci.* 39, 527–542.
 762 <https://doi.org/10.1016/j.tins.2016.06.003>
- 763 Luke, S.G., 2017. Evaluating significance in linear mixed-effects models in R. *Behav. Res.*
 764 *Methods* 49, 1494–1502. <https://doi.org/10.3758/s13428-016-0809-y>
- 765 McLaren, D.G., Ries, M.L., Xu, G., Johnson, S.C., 2012. A generalized form of context-
 766 dependent psychophysiological interactions (gPPI): A comparison to standard
 767 approaches. *Neuroimage* 61, 1277–1286.
 768 <https://doi.org/10.1016/j.neuroimage.2012.03.068>
- 769 Miall, R.C., Wolpert, D.M., 1996. Forward models for physiological motor control. *Neural*
 770 *Networks*. [https://doi.org/10.1016/S0893-6080\(96\)00035-4](https://doi.org/10.1016/S0893-6080(96)00035-4)
- 771 Oldfield, R.C., 1971. The assessment and analysis of handedness: The Edinburgh inventory.
 772 *Neuropsychologia* 9, 97–113. [https://doi.org/10.1016/0028-3932\(71\)90067-4](https://doi.org/10.1016/0028-3932(71)90067-4)

- 773 Pelli, D.G., 1997. The VideoToolbox software for visual psychophysics: Transforming
 774 numbers into movies. *Spat. Vis.* 10, 437–442.
 775 <https://doi.org/10.1163/156856897X00366>
- 776 Pereira, M., Faivre, N., Iturrate, I., Wirthlin, M., Serafini, L., Martin, S., Desvachez, A., Blanke,
 777 O., Van De Ville, D., Millán, J. del R., 2020. Disentangling the origins of confidence in
 778 speeded perceptual judgments through multimodal imaging. *Proc. Natl. Acad. Sci.* 117,
 779 8382–8390. <https://doi.org/10.1073/pnas.1918335117>
- 780 Piazza, M., Izard, V., Pinel, P., Le Bihan, D., Dehaene, S., 2004. Tuning curves for approximate
 781 numerosity in the human intraparietal sulcus. *Neuron* 44, 547–555.
 782 <https://doi.org/10.1016/j.neuron.2004.10.014>
- 783 Piazza, M., Mechelli, A., Price, C.J., Butterworth, B., 2006. Exact and approximate
 784 judgements of visual and auditory numerosity: An fMRI study. *Brain Res.* 1106, 177–
 785 188. <https://doi.org/10.1016/j.brainres.2006.05.104>
- 786 Power, J.D., Barnes, K.A., Snyder, A.Z., Schlaggar, B.L., Petersen, S.E., 2012. Spurious but
 787 systematic correlations in functional connectivity MRI networks arise from subject
 788 motion. *Neuroimage* 59, 2142–2154.
 789 <https://doi.org/10.1016/j.neuroimage.2011.10.018>
- 790 Press, C., Kok, P., Yon, D., 2020. The Perceptual Prediction Paradox. *Trends Cogn. Sci.* 24, 13–
 791 24. <https://doi.org/10.1016/j.tics.2019.11.003>
- 792 Reinert, R.M., Hartmann, M., Huber, S., Moeller, K., 2019. Unbounded number line
 793 estimation as a measure of numerical estimation. *PLoS One* 14, 1–16.
 794 <https://doi.org/10.1371/journal.pone.0213102>

- 795 Rummell, B.P., Klee, J.L., Sigurdsson, T., 2016. Attenuation of responses to self-generated
796 sounds in auditory cortical neurons. *J. Neurosci.* 36, 12010–12026.
797 <https://doi.org/10.1523/JNEUROSCI.1564-16.2016>
- 798 Scott, M., Yeung, H.H., Gick, B., Werker, J.F., 2013. Inner speech captures the perception of
799 external speech. *J. Acoust. Soc. Am.* 133, EL286–EL292.
800 <https://doi.org/10.1121/1.4794932>
- 801 Serino, A., Pozeg, P., Bernasconi, F., Solcà, M., Hara, M., Progin, P., Stripeikyte, G., Dhanis,
802 H., Salomon, R., Bleuler, H., Rognini, G., Blanke, O., 2021. Thought consciousness and
803 source monitoring depend on robotically controlled sensorimotor conflicts and illusory
804 states. *iScience* 24, 101955. <https://doi.org/10.1016/j.isci.2020.101955>
- 805 Shergill, S.S., White, T.P., Joyce, D.W., Bays, P.M., Wolpert, D.M., Frith, C.D., 2013.
806 Modulation of somatosensory processing by action. *Neuroimage* 70, 356–362.
807 <https://doi.org/10.1016/j.neuroimage.2012.12.043>
- 808 Slamecka, N.J., Graf, P., 1978. The generation effect: Delineation of a phenomenon. *J. Exp.*
809 *Psychol. Hum. Learn. Mem.* 4, 592–604. <https://doi.org/10.1037/0278-7393.4.6.592>
- 810 Stripeikyte, G., Pereira, M., Rognini, G., Potheegadoo, J., Blanke, O., & Faivre, N. (2021).
811 Increased functional connectivity of the intraparietal sulcus underlies the attenuation
812 of numerosity estimations for self-generated words [Data set]. Zenodo.
813 <http://doi.org/10.5281/zenodo.4925909>
- 814 Thomas, E.R., Yon, D., Lange, F.P. de, Press, C., 2020. Action enhances predicted touch.
815 *bioRxiv* 2020.03.26.007559. <https://doi.org/10.1101/2020.03.26.007559>
- 816 Tian, X., Poeppel, D., 2010. Mental imagery of speech and movement implicates the

- 817 dynamics of internal forward models. *Front. Psychol.* 1, 1–23.
 818 <https://doi.org/10.3389/fpsyg.2010.00166>
- 819 Tian, X., Zarate, J.M., Poeppel, D., 2016. Mental imagery of speech implicates two
 820 mechanisms of perceptual reactivation. *Cortex* 77, 1–12.
 821 <https://doi.org/10.1016/j.cortex.2016.01.002>
- 822 Timm, J., SanMiguel, I., Keil, J., Schröger, E., Schönwiesner, M., 2014. Motor Intention
 823 Determines Sensory Attenuation of Brain Responses to Self-initiated Sounds. *J. Cogn.*
 824 *Neurosci.* 26, 1481–1489. https://doi.org/10.1162/jocn_a_00552
- 825 Tzourio-Mazoyer, N., Landeau, B., Papathanassiou, D., Crivello, F., Etard, O., Delcroix, N.,
 826 Mazoyer, B., Joliot, M., 2002. Automated anatomical labeling of activations in SPM
 827 using a macroscopic anatomical parcellation of the MNI MRI single-subject brain.
 828 *Neuroimage* 15, 273–289. <https://doi.org/10.1006/nimg.2001.0978>
- 829 Ullsperger, M., Harsay, H.A., Wessel, J.R., Ridderinkhof, K.R., 2010. Conscious perception of
 830 errors and its relation to the anterior insula. *Brain Struct. Funct.* 214, 629–643.
 831 <https://doi.org/10.1007/s00429-010-0261-1>
- 832 Vaccaro, A.G., Fleming, S.M., 2018. Thinking about thinking: A coordinate-based meta-
 833 analysis of neuroimaging studies of metacognitive judgements. *Brain Neurosci. Adv.* 2,
 834 239821281881059. <https://doi.org/10.1177/2398212818810591>
- 835 van de Ven, V., Esposito, F., Christoffels, I.K., 2009. Neural network of speech monitoring
 836 overlaps with overt speech production and comprehension networks: A sequential
 837 spatial and temporal ICA study. *Neuroimage* 47, 1982–1991.
 838 <https://doi.org/10.1016/j.neuroimage.2009.05.057>

- 839 Whitford, T.J., 2019. Speaking-Induced Suppression of the Auditory Cortex in Humans and
840 Its Relevance to Schizophrenia. *Biol. Psychiatry Cogn. Neurosci. Neuroimaging* 4, 791–
841 804. <https://doi.org/10.1016/j.bpsc.2019.05.011>
- 842 Whitford, T.J., Jack, B.N., Pearson, D., Griffiths, O., Luque, D., Harris, A.W.F., Spencer, K.M.,
843 Le Pelley, M.E., 2017. Neurophysiological evidence of efference copies to inner speech.
844 *Elife* 6, 1–23. <https://doi.org/10.7554/eLife.28197>
- 845 Wolpert, D.M., Flanagan, J.R., 2001. Motor prediction. *Curr. Biol.* 11, 729–732.
846 [https://doi.org/10.1016/s0960-9822\(01\)00432-8](https://doi.org/10.1016/s0960-9822(01)00432-8)
- 847
- 848

849 **LEGENDS OF FIGURES AND TABLES**

850 **Figures**

851 **Figure 1.** Schematic representation of the general task flow: active (top) and passive
852 (bottom) conditions consisting of instruction, word generation/listening, numerosity and
853 error estimation. Each condition was repeated 4 times per block. Auditory and visual
854 instructions were provided in French. Simulated distribution of derived behavioral
855 performance measures using numerosity and error estimation values are depicted in Figure
856 1-1.

857
858 **Figure 2.** Behavioral results. (A) Individual numerosity performance in the active (red) and
859 passive (blue) conditions. A value of zero represents ideal performance, where the reported
860 and actual number of words match. Each dot represents a participant mean numerosity
861 performance. Grey lines connect performance from the same participant across conditions.
862 (B) Mixed-effects linear regression between numerosity estimation (reported number of
863 words) and an actual number of words. Reference dashed line with a slope equal to 1
864 represents ideal performance. Thick lines represent the global model fit, while thin lines
865 depict individual estimates. Individual plots are depicted in Figure 2-1. (C) Mean slope
866 coefficient estimates with 2.5% and 97.5% confidence intervals.

867 **Figure 3.** Percentage of simulated accurate numerosity estimations (occurrences of value
868 10) in normal distribution centred on 10 with varying standard deviation. Simulation was
869 iterated 10000 times. Reference dashed line of 19.5% absolute numerosity estimations
870 accuracy (as observed in the experiment empirical data) occurs with the standard deviation

871 of 2. Each dot represents a single iteration of the data simulation (overlapping dots are
872 depicted in higher color intensity).

873 **Figure 4.** Neural correlates of numerosity performance. (A) Main effect (active+passive
874 conditions) of the parametric modulation of numerosity performance during numerosity
875 estimation in the right intraparietal sulcus (IPS, depicted in green). (B) Box plot of the
876 corresponding individual beta estimates in the right IPS. Each dot represents a participant
877 mean beta estimates. Grey lines connect beta estimates from the same participant across
878 conditions. (C) Overlap between the parametric modulation of numerosity performance
879 during numerosity estimation (depicted in green) main effect (active + passive conditions) at
880 the lower statistical threshold of peak level uncorrected $p < 0.005$ (exploratory analyses) and
881 parametric modulation of performance monitoring during the error estimation (active vs.
882 passive condition) (depicted in purple); peak level uncorrected $p < 0.001$.

883

884 **Figure 5.** PPI analysis: numerosity estimation. (A) Increased functional connectivity in the
885 active vs. passive condition between the right intraparietal sulcus seed (IPS, depicted in
886 green) and bilateral supplementary motor area (SMA), left inferior parietal lobule (IPL) and
887 superior temporal gyri (STG), depicted in red. (C) Box plots of the corresponding beta
888 estimates for each significant PPI cluster. Each dot represents a participant mean beta
889 estimates. Grey lines connect beta estimates from the same participant across conditions.

890

891 **Figure 6.** Neural correlates of performance monitoring. (A) Decreased neural activity during
892 the active vs. passive condition in the right putamen and insula bilaterally (depicted in blue).

893 Increased activity in the active vs. passive condition in the left caudate nucleus (depicted in
 894 red). (B) Box plots of the corresponding beta estimates in the active (red) and passive (blue)
 895 conditions for each significant cluster observed. Each dot represents a participant mean
 896 beta estimates. Grey lines connect beta estimates from the same participant across
 897 conditions.

898

899 **Figure 7.** Parametric modulation of performance monitoring. (A) Positive association
 900 between the trial-wise performance monitoring and BOLD signal during performance
 901 monitoring in the active vs. passive condition in the left intraparietal sulcus (IPS, depicted in
 902 purple). (B) Box plot of corresponding beta estimates in the left IPS in the active (blue) and
 903 passive (red) conditions. Each dot represents a participant mean beta estimates. Grey lines
 904 connect beta estimates from the same participant across conditions.

905 **Tables**

906 **Table 1.** Numerosity estimation: difference between active and passive conditions. Brain
 907 areas showing a difference in activity between the active and passive condition during the
 908 numerosity estimation phase, independent of parametric modulation. The activation
 909 clusters of numerosity estimation main effect are detailed in Table 1-1. Voxel level $p < 0.001$
 910 uncorrected, cluster threshold at $p < 0.05$ FWE corrected. BA – Broadmann area, k – cluster
 911 size, R – right hemisphere, L – left hemisphere, R – right hemisphere

912

913 **Table 2.** Parametric modulation of numerosity performance (exploratory analyses at lower
 914 statistical threshold). Brain areas in which the BOLD signal correlates with the trial-by-trial

915 behavioral measures of numerosity performance during the numerosity estimation phase.
 916 Voxel level $p < 0.005$ uncorrected, cluster threshold at $p < 0.05$ FWE corrected. BA –
 917 Broadmann area, k – cluster size, R – right hemisphere, L – left hemisphere

918

919 **Table 3.** PPI analysis: numerosity estimation. Brain areas identified through PPI analysis
 920 seeding from the right intraparietal sulcus during numerosity estimation. Voxel level
 921 $p < 0.001$ uncorrected, cluster threshold at $p < 0.05$ FWE corrected. BA – Broadmann area, k –
 922 cluster size, R – right hemisphere, L – left hemisphere

923

924 **Table 4.** Error estimation: difference between active and passive conditions. Brain areas
 925 showing a difference in activity between the active and passive condition during the error
 926 estimation phase, independent of parametric modulation. The activation clusters of error
 927 estimation main effect are detailed in Table 4-1. Voxel level $p < 0.001$ uncorrected, cluster
 928 threshold at $p < 0.05$ FWE corrected. BA – Broadmann area, k – cluster size, R – right
 929 hemisphere, L – left hemisphere

930

931 **Extended data legends**

932 **Figure 1-1.** Data simulation of behavioral performance measures. Data was simulated with
 933 pseudorandom generation of an actual number of words and numerosity estimations
 934 ranging between 5 and 20. Error estimation varied between 0 and 5 as set during the task
 935 design. (A) Simulated numerosity performance. Increasing intensity of red represent linear
 936 increase of overestimation (positive values of numerosity performance), while increasing

937 intensity in blue represent linear increase of underestimation (negative values of
 938 numerosity performance). (B) Simulated performance monitoring when the number of
 939 words is constant (10 or 15 words). The performance monitoring value is depicted in the
 940 heatmap changing from blue (being correct) to red (worse performance monitoring).

941

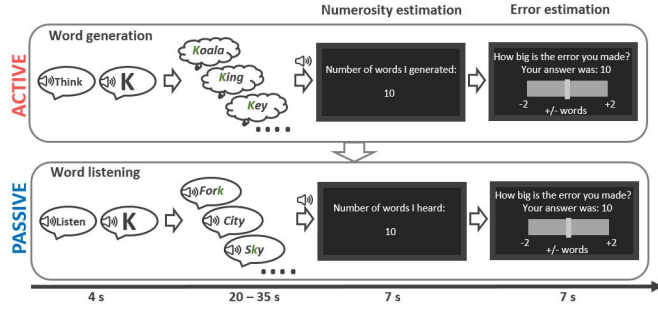
942 **Figure 2-1.** Mixed-effects linear regression between numerosity estimation (reported
 943 number of words) and an actual number of words depicted for each participant. Reference
 944 dashed line with a slope equal to 1 represents ideal performance. Thick lines represent the
 945 individual model fit per condition (active: red and passive: blue). Each dot represents a
 946 participant's single trial performance (overlapping dots are depicted in higher color
 947 intensity).

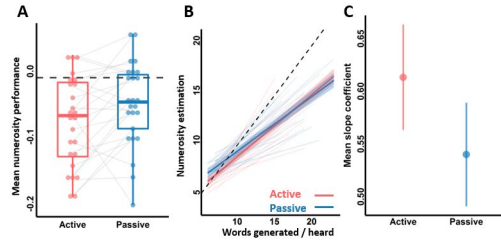
948

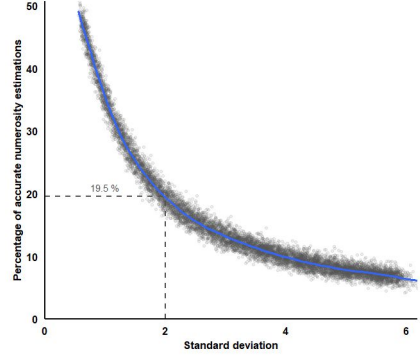
949 **Table 1-1.** Numerosity estimation: main effect (active + passive conditions). Brain areas
 950 activated during the numerosity estimation phase independent of parametric modulation.
 951 Voxel level $p < 0.001$ uncorrected, cluster threshold at $p < 0.05$ FWE corrected. BA –
 952 Broadmann area, k – cluster size, R – right hemisphere, L – left hemisphere, R – right
 953 hemisphere

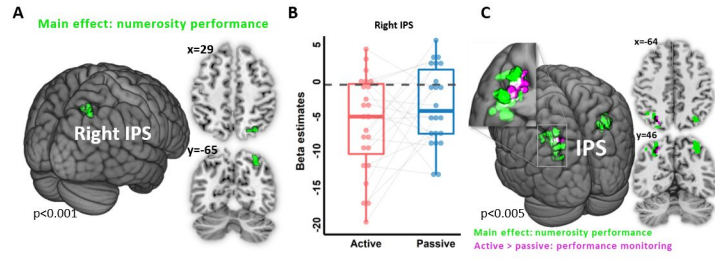
954

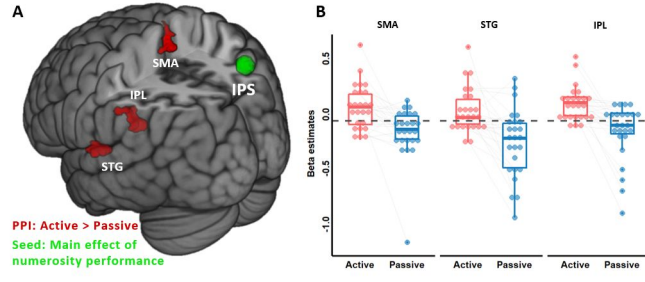
955 **Table 4-1.** Error estimation: main effect (active + passive conditions). Brain areas with
 956 activations during the error estimation phase, independent of parametric modulation. Voxel
 957 level $p < 0.001$ uncorrected, cluster threshold at $p < 0.05$ FWE corrected. BA – Broadmann
 958 area, k – cluster size, R – right hemisphere, L – left hemisphere, R – right hemisphere

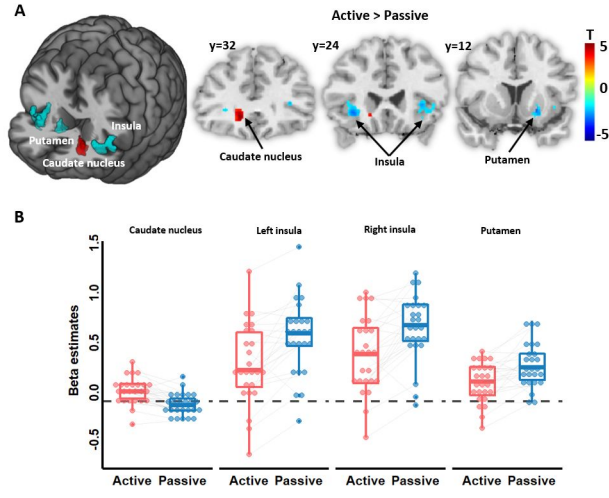


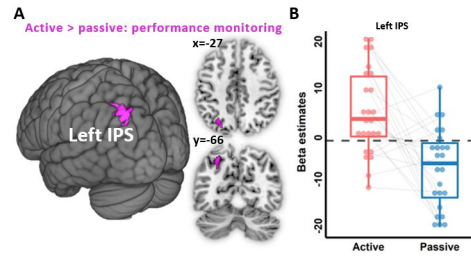












BA	Anatomical Label		k	Peak voxel MNI coordinate			p _{FWE}	T
				x	y	z		
Active < passive								
	Middle temporal g.							
	Precuneus							
	Superior temporal g.							
	Postcentral							
7	Middle cingulum							
6	Cerebellum							
40	SMA							
31	Insula							
	Precentral							
13	Supramarginal g.							
24	Angular g.							
21	Superior parietal							
4	Putamen							
32	Middle frontal g.	L/R	113587	20	8	-12	<0.001	9.75
39	Caudate							
3	Superior fontal g.							
5	Superior parietal g.							
9	Calcarine							
23	Rolandic percular							
27	Supramarginal g.							
	Thalamus							
8	Hippocampus							
18	Fusiform g.							
44	Inferior temporal g.							
	Lingual g.							
	Cuneus							
	Occipital g.							
	Thalamus	L	314	-11	-23	15	<0.001	6.84
10	Middle frontal g.	L	442	-36	50	27	0.004	4.97
10	Middle frontal g.	R	399	29	53	32	0.005	4.69

Table 1. Numerosity estimation: difference between active and passive conditions. Brain areas showing a difference in activity between the active and passive condition during the numerosity estimation phase, independent of parametric modulation. The activation clusters of numerosity estimation main effect are detailed in Table 1-1. Voxel level $p < 0.001$ uncorrected, cluster threshold at $p < 0.05$ FWE corrected. BA – Broadmann area, k – cluster size, R – right hemisphere, L – left hemisphere, R – right hemisphere

BA	Anatomical Label		k	Peak voxel MNI coordinate			p _{FWE}	T
				x	y	z		
Main effect (active + passive)								
7	Intraparietal sulcus (superior parietal g., angular g.)	R	466	29	-65	50	0.004	20
7	Intraparietal sulcus (superior/inferior parietal g., middle occipital g.)	L	758	-30	-63	42	0.000	15.9

Table 2. Parametric modulation of numerosity performance (exploratory analyses at lower statistical threshold). Brain areas in which the BOLD signal correlates with the trial-by-trial behavioral measures of numerosity performance during the numerosity estimation phase. Voxel level $p < 0.005$ uncorrected, cluster threshold at $p < 0.05$ FWE corrected. BA – Broadmann area, k – cluster size, R – right hemisphere, L – left hemisphere

BA	Anatomical Label		k	Peak voxel MNI coordinate			p _{FWE}	T
				x	y	z		
Active > passive								
41 42	Superior temporal g.	L	177	-54	-20	6	0.038	5.14
40	Inferior parietal lobule (supramarginal g., parietal inferior g.)	L	291	-44	-42	29	0.003	5.14
6	Supplementary motor area	L/R	167	-3	-30	63	0.049	4.59

Table 3. PPI analysis: numerosity estimation. Brain areas identified through PPI analysis seeding from the right intraparietal sulcus during numerosity estimation. Voxel level $p < 0.001$ uncorrected, cluster threshold at $p < 0.05$ FWE corrected. BA – Broadmann area, k – cluster size, R – right hemisphere, L – left hemisphere

BA	Anatomical Label		k	Peak voxel MNI coordinate			p _{FWE}	T
				x	y	z		
Active > passive								
	Caudate nucleus	L	336	-15	30	-6	0.004	5.76
Active < passive								
45	Insula, inferior frontal g. triangular part	L	392	-33	24	-6	0.002	5.3
47								
13								
	Putamen	R	209	20	12	-6	0.043	5.2
13	Insula, inferior frontal g. triangular part	R	482	32	27	0	0.000	4.3
47								
45								

Table 4. Error estimation: difference between active and passive conditions. Brain areas showing a difference in activity between the active and passive condition during the error estimation phase, independent of parametric modulation. The activation clusters of error estimation main effect are detailed in Table 4-1. Voxel level $p < 0.001$ uncorrected, cluster threshold at $p < 0.05$ FWE corrected. BA – Broadmann area, k – cluster size, R – right hemisphere, L – left hemisphere